RSC Advances

ROYAL SOCIETY OF CHEMISTRY

www.rsc.org/advances

Microwave Assisted Decoration of Titanium Oxides Nanotubes With $CuFe_2O_4$ Quantum Dots for Solid Phase Extraction of Uranium

W. I. Mortada [a *], A. F. Moustafa [b], A. M. Ismail [c], M.M. Hassanien [d], A. A. Aboud [e,f]

[a] Urology and Nephrology Center, Mansoura University, Mansoura, Egypt.

[b] Environmental Screening, Environmental Management Unit, Beni-Suef Governorate, Egypt.

[c] Technological & Industrial Development Sector, Ministry of Industry, Trade & S&M Projects, Cairo, Egypt

[d] Chemistry Department, Industrial Education College, Beni-Suef University, Beni-Suef, Egypt.

[e] Physical department, Faculty of Science, Beni-suef Uuniversity, Beni-Suef, Egypt.

[f] Physical department, Faculty of Science, El-Baha University, Saudi Arabia

***Corresponding author**

E-Mail: w.mortada@yahoo.com

Telephone: +2 01022772144

Fax: +2 050 2202717

Abstract

Titanium oxides nanotubes (TiO_xNTs) were prepared using a hydrothermal method followed by ion exchange and phase transformation. The obtained TiO_xNTs were decorated with $CuFe_2O_4$ quantum dots by assisted microwave procedures. The prepared nanomaterials were characterized by XRD, TEM, and IR spectroscopy. The decorated nanotubes ($DTiO_xNTs$) were used as an adsorbent for the removal of U(VI) from aqueous solutions prior to its determination by inductively coupled plasma-optical emission spectrometry. Experimental parameters including pH, contact time and amount of adsorbent were investigated by batch mode. Optimum sorption of U(VI) ions obtained at pH 6-8. The maximum adsorption capacity of $DTiO_xNTs$ towards U(VI) was found to be 366 mg g^{-1} which is better than that obtained by using TiO_xNTs (277 mg g^{-1}). The equilibrium adsorption isotherm of U(VI) was fitted with the Langmuir adsorption model. Moreover, a mini-column packed with $DTiO_xNTs$ was used for column-mode extraction and preconcentration of U(VI). Effects of layer thickness, sample volume, sample flow rate and eluent conditions were studied. Under the optimized column procedures, the preconcentration factor for U(VI) was 200. The 3σ detection limit and 10σ quantification limit were found to be 0.12 and 0.40 ng mL^{-1}, respectively. The calibration curve was linear up to 1500 ng mL^{-1}. The proposed method showed good performance in analyzing water samples of different sources and soil sample digests collected from agriculture land near an industrial area.

Key words:

Titanium oxides nanotubes decorated with $CuFe_2O_4$; Solid phase extraction; Uranium(VI); ICP-OES; soil and water samples.

1. Introduction

Uranium is a strategic element because of its industrial applications especially in the production of nuclear energy.[1] Naturally it can be found in very small amount in soils, rocks, air and water. However, significant quantities of uranium have released into the environment through the industrial activities. Additionally, contamination may be caused by catalysts, staining pigments, burning of fossil fuels and the manufacture and use of phosphate fertilizers that contain uranium.[2-4]

Uranium and its compounds are highly toxic and can cause adverse health effects to human depending on the way of exposure.[5] Ingestion of uranium can attack the kidneys. The major target is the renal proximal tubule[6], but the glomeruli may also be affected.[7] The most serious health hazard associated with the uranium is lung cancer, which is due to the inhalation of radon, a product of uranium decay.[8] Chronic uranium exposure may also result in neurotoxicity.[9]

Several techniques have been used for the determination of uranium such as alpha-spectrometry[10], inductively coupled plasma optical emission spectrometry (ICP-OES)[11-14], inductively coupled plasma mass spectrometry (ICP-MS)[15,16], X-ray fluorescence spectrophotometry (XRF)[17], neutron activation[18] and spectrophotometery.[19-22] The low concentrations of uranium in the real samples as well as the matrix interference hinder the determination of uranium by these techniques, so a separation/preconcentration step is required before the determination. For this purpose, various procedures have been used, such as solid-phase extraction (SPE)[11-22], liquid–liquid extraction[23], cloud point extraction[24], ion exchange[25], flotation[26] and extraction chromatography.[27] Solid phase extraction (SPE) has many advantages over the other separation procedures, including simplicity, higher enrichment factors, low cost, lower consumption of toxic chemicals.[28]

Nano-adsorbents have significant interest within the scientific community owing to their special properties, such as their large surface areas and high adsorption capacity.[29,30] Among these adsorbents, TiO_2 nanostructures has great advantages due to its physical and chemical stability, comparatively lower cost, non-toxicity and large surface area thence nano-TiO_2 is a good choice for SPE and modification of its surface sometimes results in enhancements of its properties.[31,32] Decoration of TiO_2 nanotubes with nanoparticles is considerably used to improve their properties such as changing the surface band bending, creation of suitable surface states that promote charge transfer with surroundings, enhancement of catalytic effects for chemical reactions.[33]

In the present study, decorated titanium oxides nanotubes with $CuFe_2O_4$ quantum dots ($DTiO_xNTs$) were prepared and characterized. The sorption behavior of $DTiO_xNTs$ toward U(VI) was investigated in both batch and column procedures. The decorated nanotubes were used as sorbents in the SPE of U(VI) from water and soil samples.

2. Experimental

2.1. Reagents and chemicals

Unless stated, all chemicals used were analytical reagent grade and purchased from Merck (Darmstadt, Germany). All solutions were prepared in deionized water that had been obtained by Milli-Q water purification system (Millipore, Billerica, MA, USA). The laboratory glassware was kept overnight in 10% v/v HNO_3 solution. Before the use, the glassware was washed with deionized water and dried in a dust free environment. Stock standard solution of U(VI) was prepared by dissolving the appropriate amounts of $UO_2(NO_3)_2.6H_2O$ in 0.5 mol L^{-1} HNO_3, and then diluted to the desired volume. The solution was standardized gravimetrically using 8-

hydroxyquinoline.[34] Working solutions were prepared daily from the stock solution by dilutions with deionized water.

2.2. Instrumentation

Determination of U(VI) was performed using inductively coupled plasma optimal emission spectrometer (ICP-OES) Perkin Elmer Model Optima 8300. The selected operating conditions of ICP-OES is presented in Table 1. The solution pH was adjusted using digital pH meter (Hanna instrument model HI 8519, Italy). Digestion of soil samples was carried out in a CEM MDS 2000 microwave digestion system (Matthews, NC, USA).

2.3. Synthesis of DTiO$_x$NTs

TiO$_x$NTs were prepared as previously described.[35] Five grams of commercial TiO_2 nanopowder (rutile phase) was dispersed in 150 mL of 10 M NaOH and stirred for 15 min till the milk like suspension was obtained. The dispersion was then transferred to a Teflon lined autoclave kept at 150 ^oC for 144 h. A white precipitate ($Na_2Ti_3O_7$) was obtained; this precipitate was washed with 1 mol L^{-1} HCl to neutralize the excess NaOH. The obtained TiO$_x$NTs where immersed in mixture of $CuCl_2.2H_2O$ and $FeCl_3.6H_2O$ solution with molar ratio 1:2, respectively. The mixture then turned into microwave operating at a power of 1200 W for 18 min.

2.4. Characterization of the nano sorbent

Fourier transform infrared (FTIR) spectrum was measured on SHIMADZU FTIR-8101 system (Shimadzu, Kyoto, Japan) in the range of 4000 to 400 cm^{-1}. Calibration of the frequency reading was made with polystyrene film. The X-ray diffraction (XRD) spectrum (Brukur 8 advance, CuK, target with secondary monochromator λ_υ = 40, mA = 40, Germany) was applied to identify the phase formation and crystal size. The size and morphology of the synthesized nanomaterial

were investigated using JEOL transmission electron microscope (TEM) 2100 high resolution transmission electron microscope (JEOL Ltd., Tokyo, Japan).

2.5. Sorption experiments

2.5.1. Batch mode

In 250 Erlenmeyer flask, 100 mL aliquots of aqueous solution containing suitable amount of U(VI) were taken and adjusted to a desired pH (3-9). Accurately weighed amount of $DTiO_xNTs$ (2-100 mg) were added and the mixture was stirred using magnetic stirrer for a fixed period of time (15 min-24 h). Then, $DTiO_xNTs$ were separated by filtration. The % removal of U(VI) by $DTiO_xNTs$ was calculated by the following formula:

$$\% \, \boldsymbol{Removal} = \frac{(\boldsymbol{C_i} - \boldsymbol{C_e})}{\boldsymbol{C_i}} \, \mathbf{x\ 100}$$

where C_i and C_e are the initial and equilibrium concentration of U(VI) (mg/L), respectivelly.

Al tests were conducted in triplicate at room temperature and their mean values were used in the calculations.

2.5.2. Sorption isotherm

Sorption isotherm was obtained by equilibrating 20 mg of $DTiO_xNTs$ with U(VI) (pH 6) of different initial concentrations for 4 h. After separation, the final concentrations of U(VI) in the solutions were measured by ICP-OES. The amount of U(VI) adsorbed per gram of $DTiO_xNTs$ was calculated using the following equation:

$$\boldsymbol{q_e} = \frac{(\boldsymbol{C_i} - \boldsymbol{C_e})\boldsymbol{V}}{\boldsymbol{m}}$$

where q_e represents the adsorption capacity (mg g^{-1}), C_i and C_e are the initial and equilibrium concentrations of the metal ions (mg L^{-1}), m is the mass of HAPNR (g), and V is the volume of solution (L).

2.5.3. Column mode

One hundred mg of $DTiO_xNTs$ was slurried in deionized water and then packed into a 70 mm × 6 mm (i.d.) polyethylene microcolumn. The ends of the column were fitted with a small portion of glass wool to keep the nanosorbent inside of the column and to prevent the loss of $DTiO_xNTs$ during the sampling. The column has a 50 mL reservoir. The flow of sample and eluent solutions through the column was controlled with a peristaltic pump. Prior to use, the column was preconditioned with buffer solution at pH 6.0. After each experiment, the column was rinsed three times with 10 mL of deionized water and stored for further use. The sample solution (100-1000 mL), buffered at pH 6, was passed through the column at a flow rate of 2.5 mL min^{-1}. The retained metal ions were eluted with 5.0 mL of 0.5 mol L^{-1} of HCl at a flow rate of 2 mL min^{-1}. The effluent was analyzed for U(VI) content by ICP-OES.

2.6. Real samples

Water samples were filtered through a 0.45 μm pore sized Millipore cellulose nitrate membrane, acidified to pH 1 with HNO_3 and stored in a refrigerator in a dark polyethylene bottle until analysis. Twelve soil samples were collected from agricultural land near Abu-Zaabal fertilizer's factory at 20-50 cm from the surface. The samples were dried at 90 ^oC for 2 h, ground, passed through a sieve of 120 meshes and homogenized. Five milliliters of concentrated HNO_3, 2 mL of concentrated HF and 2 mL of deionized water were added to 0.5 g of the sample in a Teflon vessel. The microwave system was operated as follow: 2 min at 8 atm and 600W; 3 min at 12 atm and 800W; 8 min at 16 atm and 800W.[36] Finally, 20 mL of 5% w/v boric acid was added, to neutralize excess HF, and the solution was filtered and brought to a final volume of 50 mL with deionized water.

3. RESULTS AND DISCUSSION

3.1. Characterization of raw and TiO_xNTs

Fig (1a,b) show the XRD pattern of TiO_2 powder and prepared TiO_xNTs, respectively. It was obtained from Fig. 1a that the raw material is pure rutile phase of TiO_2 powder with crystal size of 93 nm and high crystallinity. As a result of thermal treatment process of TiO_2 powder different oxides of sodium titanium and titanium oxide nanotubes were formed with low crystallinity (as illustrated in Fig 1b).

TEM analysis was used for particles size determination and to study the morphology of the obtained nanotubes. Fig 2 illustrates TEM of prepared TiO_x nanotubes, it can be deduced that the obtained TiO_x nantubes have uniform, hollow and layered structures. The geometry of the obtained nanotubes was measured to be 5 nm inner diameters, 9 nm outer diameter and 141 nm for the length.

3.2. Characterization of DTiO_xNTs

Fig. 3 shows the XRD patterns of DTiO_xNTs. It can be illustrated that; the formed phases are sodium titanium oxide ($Na_2Ti_3O_7$), sodium iron oxide ($Na_4Fe_2O_5$) and Landauite phase of titanium iron oxide ($Ti_2Fe_2O_7$) with no evidence for presence of $CuFe_2O_4$ or CuO_x nanoparticles. The absence of $CuFe_2O_4$ or CuO_x peaks may be attributed to high dispersion of $CuFe_2O_4$ or CuO_x on the surface and/or lattice of titanium nanotubes and / or the small portion of the formed $CuFe_2O_4$ quantum dots.[37] Semi-quantitative (SQ) analysis of XRD showed that Landauite phase of titanium iron oxide ($Ti_2Fe_2O_7$) has the highest percentage (37.2%) then sodium iron oxide ($Na_4Fe_2O_5$) (33.5%) finally sodium titanium oxide ($Na_2Ti_3O_7$) has the smallest percentage (29.4%). The high SQ percentage of $Ti_2Fe_2O_7$ and $Na_4Fe_2O_5$ indicate high loading percentage of iron oxides on the surface of TiO_x nanotubes. Low crystallinity may be attributed to the small crystal size and high dispersion of Q.Ds on the surface of the TiO_xNTs.[37]

Fig. 4 shows TEM image of $DTiO_xNTs$, as shown the decoration process take place on the outer surface of the nanotubes which suggesting the successful loading process. The decorating nanoparticles have cubic shape with quantum size of 6 nm. Also it can be observed that the nanotubes still save their tubular form which indicating that microwave assisted the decoration of the nanotubes without distorting.

The vibrational spectrum of a molecule is considered to be a unique physical property and is characteristic of the molecule. As such, the infrared spectrum can be used as a fingerprint for identification by comparing the unknown spectrum with previously recorded reference spectra. The exact band position depending on the chemical composition of the sample as well as calibration and resolution of the instrument. FT-IR spectrum is useful to study the surface chemical structure of the sample. Fig. 5 shows FT-IR spectrum of $DTiO_xNTs$ recorded at the range of 4000 to 400 cm^{-1}. The two main metal oxygen bands appears between 600-400 cm^{-1} is observed which arises the vibration of ions in the crystal lattices of ferrites compounds.[38] The absorption band at 462.8 cm^{-1} attributed to octahedral sites of Cu cations in $CuFe_2O_4$ Q.Ds (Cu-O), while their vibration band appears at 440 cm^{-1}.[39] On the other hand the observed absorption band at 544.8 cm^{-1} may be attributed to the intrinsic vibrations of the tetrahedral metal complexes (Fe-O).[38,40] It was concluded that the disappearance of absorption band 510 cm^{-1} in the Fe/Ti mixed oxide is due to the formation of pseudobrookite phase (Fe_2TiO_5) where Fe^{3+} is dispersed in to the lattice of TiO_xNTs which confirm the low crstallinty obtained from XRD.[41] The band at 700-500 cm^{-1} corresponding to the vibration of the Ti-O bonds in the TiO_x lattice. [42] The shift in the lower of the O-Ti-O band width increase may be assumed to the decreasing in size of the nanoparticles. The broad band at 3359 cm^{-1} due to the presence of surface OH group (adsorbed water) which corresponding to stretching vibrations of OH groups.

3.3. Batch experiments

3.3.1. Effect of contact time

The influence of contact time on the removal of U(VI) by $DTiO_xNTs$ is studied under the following conditions: 100 mL solution, 100 mg L^{-1} U(VI), pH 6, 25 mg $DTiO_xNTs$. The contact time varies from 15 min to 24 h, as presented in Fig. 6a. It suggested that the adsorption process occurred in two phases: a quick phase, followed by a slow increase until the equilibrium was reached. After 4 h, the % removal of U(VI) stays constant with no obvious changes. Therefore, the adsorption equilibrium time considered for the further work is set to be 4 h.

3.3.2. Effect of pH

pH is one of the most significant factors affecting the metal ion adsorption process. Thus, the effect of pH on adsorption capacity was studied over a range of pH values from 3 to 9. The pH of the solution was adjusted to the required value by the addition of 0.05 mol L^{-1} NaOH and/or 0.05 mol L^{-1} HNO_3. As depicted in Fig. 6b, the adsorption of U(VI) on $DTiO_xNTs$ increased when pH increased from 3 to 6 and approaches a plateau at pH range of 6-8. At a lower pH (3-5), there is a competition between H^+ ions with U(VI) for the binding sites on the sorbent surface resulting in a decrease in the adsorption capacity.[43] As the pH increases (6-8), deprotonation occurs and the surface of the adsorbent becomes negatively charged, so that the electrostatic attraction between adsorbent and U(VI) probably supports the interaction between each other. However, at higher pH (> 8), the adsorption is reduced due to the formation of uranyl complexes such as UO_2OH^+, $(UO_2)_2(OH)_2^{2+}$ and $(UO_2)_3(OH)_5^+$. [44] So a pH of 6 was chosen for the further experiments.

3.3.3. Effect of the amount of adsorbent

The effect of amount of $DTiO_xNTs$ on the removal of U(VI) was examined by varying the amounts of $DTiO_xNTs$ in the range of 2.0-100.0 mg. The results were shown in Fig. 6c. As can

be seen, the extraction of U(VI) was quantitative by using 10.0 mg of $DTiO_xNTs$. Subsequent extraction experiments were carried out with 20.0 mg of $DTiO_xNTs$ in order to ascertain high capacity and account for other extractable species.

3.4. Sorption isotherm

The sorption isotherm of U(VI) ions on $DTiO_xNTs$ is shown in Fig. 7a. As shown, with the increase of U(VI) concentration, the sorption capacities first increase sharply, then increase slowly, and finally reach saturation. To gain a better understanding of sorption mechanism, Langmuir model is used to express the experimental data. Langmuir equation is based on the assumption of ideal and uniform monolayer adsorption.[45] The general form of the Langmuir isotherm is

$$\frac{C_e}{q_e} = \frac{C_e}{q_m} + \frac{1}{bq_m}$$

where C_e (mg L^{-1}) is the equilibrium metal concentration, q_e (mg g^{-1}) denotes the amount of metal ion sorbed per unit weight of $DTiO_xNTs$, q_m (mg g^{-1}) means the maximum sorption capacity of the surface and b (L mg^{-1}) indicates the adsorption constant related to bonding-energy of the adsorbate to the adsorbent. The constants b and q_m can be determined from the slope and intercept of the linear plot C_e versus C_e/q_e. The results (Fig. 7b) showed that the value of correlation coefficient for the adsorption of U(VI) onto $DTiO_xNTs$ was 0.9972, which demonstrated the good fitting of experimental data by this model. The Langmuir constant for U(VI) was 0.164 L mg^{-1}. The q_m value for the adsorption of U(VI) by $DTiO_xNTs$ was 366 mg g^{-1}. Table 2 displays a comparison of the maximum sorption capacity of $DTiO_xNTs$ with that of other sorbents, [46-52] indicating the excellent sorption abilities of $DTiO_xNTs$ toward U(VI). The results presented in Table 2 also illustrated that $DTiO_xNTs$ has better U(VI) adsorption capacity

than TiO_xNTs. This denotes that the decoration of TiO_xNTs with $CuFe_2O_4$ enhances the adsorption activity to U(IV).

The Langmuir isotherm can be expressed in terms of a dimensionless constant named separation factor or equilibrium parameter, R_L which is defined as:

$$R_L = \frac{1}{1 + bC_i}$$

where C_i is the initial metal concentration. The value of R_L indicates the type of isotherm to be favorable ($0 < R_L < 1$), unfavorable ($R_L > 1$), linear ($R_L = 1$), or irreversible ($R_L = 0$).[53] From our study, R_L values for U(VI) adsorption was 0.0296. This, for an initial metal ions concentration of 200 mg L^{-1}, therefore, the adsorption process is favorable.

3.5. Column experiments

3.5.1. Effect of layer thickness

The effects of the column ped thickness of $DTiO_xNTs$ for the adsorption of U(VI) were studied in the range of 5-50 mm at flow rate of 2.5 mL min^{-1}. As can be seen in Fig. 8, increasing the thickness of the layer result in an increment in the adsorption of U(VI). This may be due to an increase of the surface area of adsorbent that provided more binding sites for adsorption of U(VI) with a thicker layer and the efficiency is increased by allowing sufficient time for the U(VI) adsorbate to diffuse into the whole mass of the adsorbent. The removal of U(VI) was quantitative and constant when 20-50 mm ped thickness was used. Therefore, a ped thickness of 22 mm (equivalent to 100 mg $DTiO_xNTs$) was chosen as the optimal.

3.5.2. Effect of flow rate

The flow rate of the sample solutions through the packed column is one of the main factors in SPE, by reducing the flow rate; the recovery and the separation time are increased. To obtain quantitative recovery and decrease the analysis time, this parameter should be optimized. 100

mL solution containing of 25.0 ng mL^{-1} of U(VI) was loaded through the column packed with $DTiO_xNTs$ at different flow rates in the range of 0.5-10.0 mL min^{-1}. The other column parameters were kept constant. The obtained results implied that the sorption of U(VI) was maximum up to the sample flow rate of 2.5 mL min^{-1}. Therefore, in the other experiments, the sample flow rate of 2.5 mL min^{-1} was used.

3.5.3. Effect of type, concentration and volume of eluent

To select the most efficient eluent, different desorbing agents were used to find the best desorbing solution for the adsorbed U(VI) from the column. Various solutions, with different concentrations and volumes, such as HNO_3, HCl, and acetic acid were examined as eluent. The results in Table 3 shows that the maximum recoveries are obtained only when 5 mL of 0.5 mol L^{-1} HCl is used as an eluent.

3.5.4. Effect of eluent flow rate

The effect of flow rate of the eluent (0.5 mol L^{-1} HCl) on desorption of U(VI) (ng mL^{-1}) from $DTiO_xNTs$ was studied in range of 0.5-5 mL min^{-1}. The analyte was desorbed completely at an eluent flow rate of less than 2 mL min^{-1}. Thus, an eluent flow rate of 2.0 mL min^{-1} was employed for subsequent investigations.

3.5.5. Breakthrough volume

To study the effect of sample volume on the recovery of U(VI) by the recommended column procedure, the sample solutions in the range of 100‑1000 mL containing 25 ng mL^{-1} of U(VI) were operated and eluted using 5.0 mL of 0.5 mol L^{-1} HCl. It was found that the analytes quantitatively was enriched on $DTiO_xNTs$ without significant change in their efficiency until 1000 mL. Consequently, a preconcentration factor of 200 could be attained when the sample volume was 1000 mL. The high sample throughout that was obtained in this study is related to

various factors such as high surface area of the sorbent and presence of effective functional groups in its structure.

3.5.6. Interference study

To study the influence of various ions and some organic compounds on the determination of U(VI), 100 mL solution containing 25 ng mL^{-1} U(VI) was mixed with the interfering species and subjected to the recommended column procedure. The limit of tolerance is defined as the amount of electrolyte ions causing an error of 5% in the recovery of U(VI). The results in Table 4 show that most of the examined species do not interfere with the determination of U(VI) by the proposed procedures, and many of them are tolerated at high levels.

3.5.7. Reusability of the nanosorbent

Reusability of sorbent is one of the important factors in evaluating the long-term performance of the sorption materials. For this purpose, sorption-desorption cycles were repeated for 8 times by using the same sorbent. The results showed that $DTiO_xNTs$ is stable in operation process without losing its significant sorption capacities and decreasing in the recoveries of U(VI).

3.6. Analytical performance

The limit of detection (LOD), limit of quantitation (LOQ), precision, accuracy, linear range and regression equation were used to evaluate the presented method for quantification of U(VI). LOD and LOQ for U(VI) were determined using the column procedure by passing a blank solution through $DTiO_xNTs$ under the optimal experimental conditions. According to the definition of IUPAC, the LODs ($3S_b$) of this procedure was 0.12 ng mL^{-1}, where "S_b" is standard deviation of blank solution. The LOQs, defined as ten times of the S_b values, were calculated as 0.40 ng mL^{-1}. To monitor precision (in terms of RSD), 9 replicate standards samples containing 25 ng mL^{-1} of U(VI) were measured. The U(VI) mean concentration was found to be 24.1 ng mL^{-}

^{1} with RSD values of 2.2%. The calibration curve was linear (r^2 = 0.9964) from LOQ value up to 1500 ng mL^{-1} with the equation of $I = 4.6 \times 10^{-3}\ C + 0.028$ (where I is the intensity, and C is the concentration of U(VI) in ng mL^{-1}). The accuracy of the proposed preconcentration method was confirmed by analysis of spiked water samples. Results were tabulated in Table 5, which show the applicability of the suggested method for determination of U(VI) in real samples.

3.7. Comparison of the proposed method with other methods

A comparison of figures of merit obtained for our study and other studies using various sorbents for the preconcentration of U(VI) is given in Table 6. As seen, the limit of detection by the present method is superior or comparable to the other methods except those used ICP-MS as detection technique. The procedure is linear over a wide range of U(VI) concentrations. The feasibility of the repeated use of DTiO$_x$NTs as well as the simple way of preparation are additional advantages.

3.8. Application

As our procedure is precise and accurate, it has been used to determine U(VI) in soil samples collected from farmland near Abu Zaabal industrial area. This area is located in the north of Cairo city and involves more than 700 industrial facilities beside Abu Zaabal for special chemicals and Abu Zaabal for fertilizers and chemicals industries. There are many studies have confirmed the adverse impact of pollutants on the environment in this region.[54-58] One of these pollutants is uranium. 12 samples were collected from agricultural soils of different places in this region. All samples were treated as described in the experimental part and analyzed by the proposed procedure. As shown in Table 5, the concentration of U in the collected soil samples were ranged from 1.25 to 2.41 μg g^{-1} with a mean value of 1.97 μg g^{-1}. According to the Canadian Council of Ministers of the Environment (CCME) soil guidelines [59], concentrations

below 23 μg g^{-1} of U were suggested for agricultural and residential purposes. United Nations Scientific Committee on the Effects of Atomic Radiation [60] defined the normal concentration of U in soil as below 11.7 μg g^{-1}. Based on our results, none of the soil samples had exceeded the limits for agricultural activities. Our results confirmed that the concentration of U in the soil in this region is within the allowable level.

Conclusion

In the present study, $DTiO_xNTs$ showed a high adsorption capacity towards U(VI). This nano-sorbent was successfully applied to the separative preconcentration of trace amounts of U(VI) from aqueous solution without matrix effects. The proposed method is simple, rapid and of low analysis cost. The good analytical features of the presented method showed that it is a appropriate and promised one. The method provides good precision and high accuracy indicated by the quantitative recovery of spiked U(VI) samples. The results of this study clearly showed the importance of this method, which could apply to determination of U(VI) in real samples.

References

1 J. S. Santos, L. S. G. Teixeira, W. N. L. d. Santos, V. A. Lemos, J. M. Godoy, S. L. C. Ferreira, *Anal. Chim. Acta*, 2010, **674**, 143.

2 J. D. Wall and L. R. Krumholz, *Annu. Rev. Microbiol.*, 2006, **60**, 149.

3 E. R. Landa and T. B. Councell, *Health Phys*., 1992, **63**, 343.

4 M. Betti and L. A. Delasheras, *Spectrochim. Acta, Part B*, 2004, **59**, 1359.

5 J. Liu, R.A. Goyer, M.P. Waalkes, Toxic effects of metals, in C.D. Klaassen, (Ed.), Casarett and Doull's Toxicology, The Basic Science of Poisons, 7th ed., McGraw-Hill, New York, pp. 931-979, 2008.

6 P. Kurttio, A. Auvinen, L. Salonen, H. Saha, J. Pekkanen, I. Mäkeläinen, S. B. Väisänen, I. M. Penttilä, H. Komulainen, *Environ. Health Perspect.*, 2002, **110**, 337.

7 S. M. Pinney, R. W. Freyberg, G. E. Levine, D. E. Brannen, L. S. Mark, J. M. Nasuta, C. D. Tebbe, J. M. Buckholz, R. Wones, *Int. J. Occup. Med. Environ. Health*, 2003, **16**, 139.

8 H. Laborde-Castérot, D. Laurier, S. Caër-Lorho, C. Etard, A. Acker, E. Rage, *Occup. Environ. Med.*, 2014, **71**, 611.

9 G.C. Jiang, B. Aschner, *Biol. Trace Elem. Res.*, 2006, **110** ,1.

10 E. Manickam, S. Sdraulig, R.A. Tinker, *J. Environ. Radioactiv.*, 2008, **99**, 491.

11 S. R. Yousefi, S. J. Ahmadi, F. Shemirani, M. R. Jamali and M. S. Niasari, *Talanta*, 2009, **80**, 212.

12 A. Rezaei, H. Khani, M. M. Farahani, M. K. Rofouei, *Anal. Methods*, 2012, **4**, 4107.

13 M. R. Jamali, Y. Assadi, F. Shemirani, M. R. Milani Hosseini, R. R. Kozani, M. Masteri-Farahani, M. Salavati-Niasari, *Anal. Chim. Acta*, 2006, **579**, 68.

14 K. Oshita, K. Seo, A. Sabarudin, M. Oshima, T. Takayanagi and S. Motomizu, *Anal. Bioanal. Chem.*, 2008, **390**, 1927.

15 K. Benkhedda, V.N. Epov, R.D. Evans, *Anal. Bioanal. Chem.*, 2005, **381**, 1596.

16 F. A. Aydin, M. Soylak, *Talanta*, 2007, **72**, 187.

17 N.L. Misra, S. Dhara, K.D. Singh Mudher, *Spectrochim. Acta B*, 2006, **61**, 1166.

18 S. Landsberger, R. Kapsimalis. *J. Environ. Radioactiv.*, 2013, **117**, 41.

19 Ch. Siva Kesava Raju, M.S. Subramanian, *J. Hazard. Mat.*, 2007, **145**, 315.

20 V.K. Jain, R.A. Pandya, S.G. Pillai, P.S. Shrivastav, *Talanta*, 2006, **70**, 257.

21 Ch. Siva Kesava Raju, M.S. Subramanian, *Talanta*, 2005, **67**, 81.

22 R.S. Praveen, P. Metilda, S. Daniel, T. Prasada Rao, *Talanta*, 2005, **67**, 960.

23 A. Takahashi, Y. Ueki, S. Igarashi, *Anal. Chim. Acta*, 1999, **387**, 71.

24 C. Labrecque, S. Potvin, L. Whitty-Léveillé, D. Larivière, *Talanta*, 2013, **107**, 284.

25 A. Aziz, S. Jan, F. Waqar, B. Mohammad, M. Hakim and W. Yawar, *J. Radioanal. Nucl. Chem.*, 2010, **284**, 117.

26 M.E. Khalifa, *Sep. Sci. Tech.*, 1998, **33**, 2123.

27 M.L. Dietz, E. P. Horwitz, L. R. Sajdak, R. Chiarizia, Talanta 2001, 54, 1173.

28 V. Camel, Spectrochim. Acta Part B, 2003, 58, 1177.

29 Y Zhang, C Zhong, Q Zhang, B Chen, M He, B Hu, RSC Adv., 2015,5, 5996.

30 W. I. Mortada, I. M. M. Kenawy, A. M. Abdelghany, A. M. Ismail, A. F. Donia, K. A. Nabieh, *Mat. Sci. Eng. C*, 2015, **52**, 288.

31 N. Pourreza, S. Rastegarzadeh, A. Larki, *J. Ind. Eng. Chem.*, 2014, **20**, 2680.

32 H. Zhang, S. Shuang, G. Wang, Y. Guo, X. Tong, P. Yang, A. Chen, C. Dong, Y. Qin, *RSC Adv.*, 2015,**5**, 4343.

33 K. Lee, A. Mazare, P. Schmuki, *Chem. Rev.*, 2014, **114**, 9385.

34 G. H. Jeffery, J. Bassett, J. Mendham, R. C. Denney, Vogel's Textbook of Quantitative Chemical Analysis, 5th Ed., Longman Scientific and Technical, New York, p. 474, 1989.

35 M. Bahgat, A. A. Farghali, A. F. Moustafa, M. H. Khedr, M. Y. Mohassab-Ahmed, *Appl. Nanosci.*, 2013, **3**, 241.

36 L. Moberg, K. Pettersson, I. Gustavssonb, *J. Anal. Atom. Spectrom.*, 1999, **14**, 1055.

37 Y. Yu, H-H. Wu, B-L. Zhu, S-R. Wang, W-P. Huang, S-H. Wu, S-M. Zhang, *Catal. Lett.*, 2008, **121**, 165.

38 V. A. M. Brabers, *Phys. Stat. Solid,* 1969, **33**, 563.

39 M. Kanagaraj, P. Sathishkumar, G. K. Selvan, I. P. Kokila, S. Arumugam, *Indian J. pure appl. phys.*, 2014, **52**, 124.

40 R. D. Waldron, *Phys. Rev.*, 1955, **99**, 1727.

41 J. Rouquerol, D. Avnir, C. W. Fairbridge, D. H. Everett, J. M. Haynes, N. Pernicone, J. D. F. Ramsay, K. S. W. Sing, K. K. Unger, *Pure Appl. Chem.*, 1994, **66**, 1739.

42 X. Li, D. Wang, Q. Luo, J. An, Y. Wang, G. Cheng; *J. Chem. Technol. Biotechnol.*, 2008, **83**, 1558.

43 J. Song, H. Kong, J. Jang, *J. Colloid Interface Sci.*, 2011, **359**, 505.

44 L. Tan, J. Wang, Q. Liu, Y. Sun, X. Jing, L. Liu, J. Liu, D. Song, *New J. Chem.*, 2015, **39**, 868.

45 K.Y. Foo, B. H. Hameed, *Chem. Eng. J.*, 2010, **156**, 2.

46 R. Hu, D. Shao, X. Wang, *Polym. Chem.*, 2014, **5**, 6207.

47 D. D. Shao, Z. Q. Jiang, X. K. Wang, J. X. Li and Y. D. Meng, *J. Phys. Chem. B*, 2009, **113**, 860.

48 G. X. Zhao, T. Wen, X. Yang, S. B. Yang, J. L. Liao, J. Hu, D. D. Shao, X. K. Wang, *Dalton Trans.*, 2012, **41**, 6182.

49 M. Zeng, Y. Huang, S. Zhang, S. Qin, J. Li, J. Xu, *RSC Adv.*, 2014, **4**, 5021.

50 Y. G. Zhao, J. X. Li, S. W. Zhang, H. Chen. D. D. Shao, *RSC. Adv.*, 2013, **3**, 18952.

51 M. Liu, C. Chen, T. Wen, X. Wang. *Dalton Trans.*, 2014, **43**, 7050.

52 L. Tan, J. Wang, Q. Liu, Y. Sun, X. Jing, L. Liu, J. Liu, D. Song. *New J. Chem.*, 2015,**39**, 868.

53 T. W. Weber, R. K. Chakkravorti, *AIChE J.*, 1974, **20**, 228.

54 A. A. S. Ali, N. M. El Taieb, A. M. A. Hassan. Y. H. Ibrahim, S. G. Abd El Wahab, *J. Am. Sci.*, 2011, **7**, 347.

55 M. E. Goher, A. M. Hassan, I. A. Abdel-Moniem, A. H. Fahmy, S. M. El-sayed. *Egypt. J. Aquat. Res.,* 2014, **40**, 225.

56 W. M. Arafa, W. M. Badawy, N. M. Fahmi, K. Ali, M. S. Gad, O. G. Duliu, M. V. Frontasyeva, E. Steinnes. *J. Afr. Earth Sci.*, 2015, **107**, 57.

57 H. S. Ibrahim, M. A. Ibrahim, F. A. Samhan, *J. Hazard. Mater.,* 2009, **168**, 1012-1016.

58 A.H. Orabi, E.M. El-Sheikh, A.R. Mowafy, M. Abdel-Khalek, M.Y. El Kady, *Int. J. Miner. Process.*, 2015, **137**, 26.

59 CCME. Canadian soil quality guidelines for the protection of environmental and human health: summary tables. In: Canadian Environmental Quality Guidelines. CCME, Winnipeg, 2007.

60 United Nations Scientific Committee on the Effects of Atomic Radiation. Sources and effects of ionizing radiation : UNSCEAR 1993 Report to the General Assembly, with Scientific Annexes. United Nations, New York, 1993.

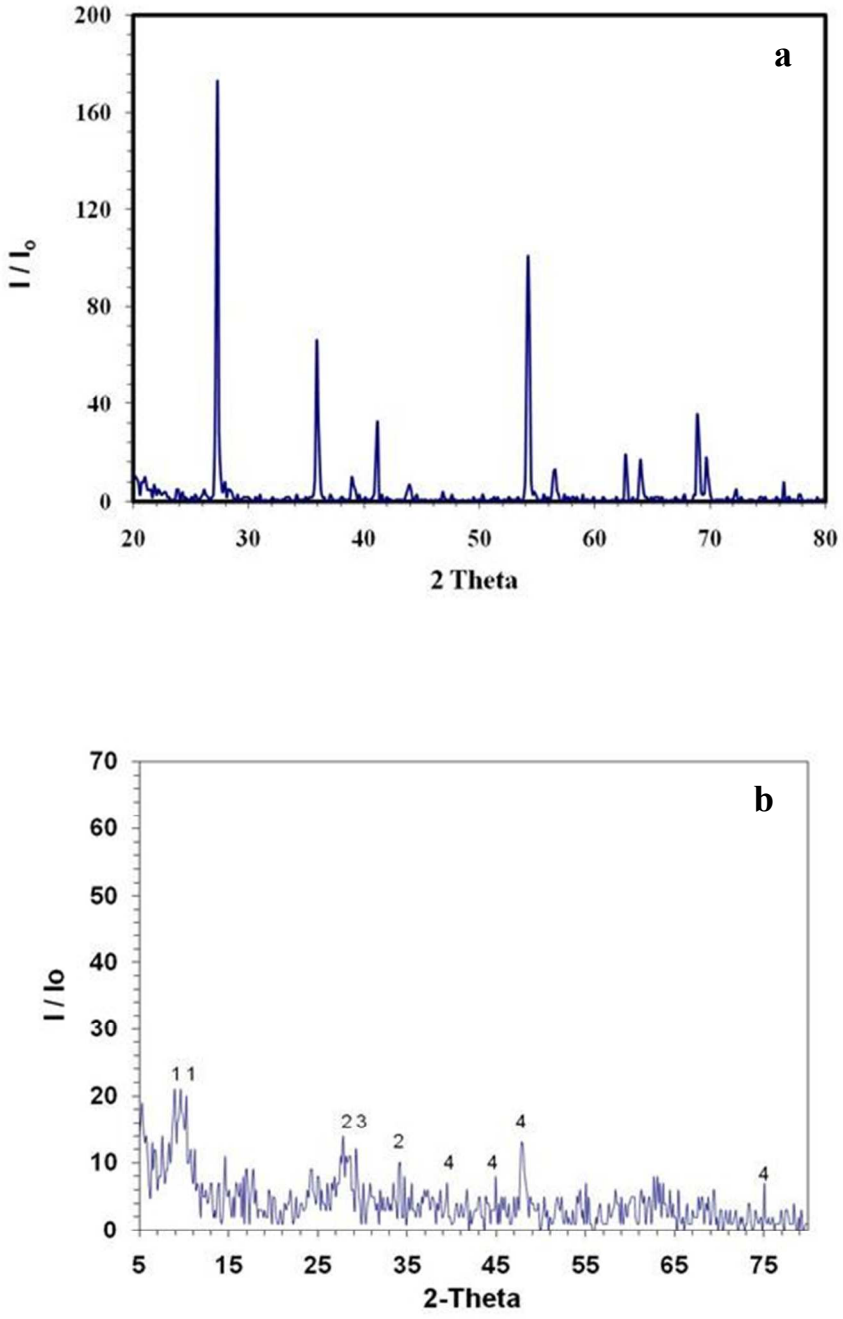

Fig. 1 XRD patterns of (a) commercial rutile phase TiO_2 nano-powder (b) titanium oxides nanotubes where, (1) $Na_2Ti_3O_7$, (2) $Na_2Ti_6O_{16}$, (3) $Na_2Ti_9O_{19}$, (4) Ti_3O_5

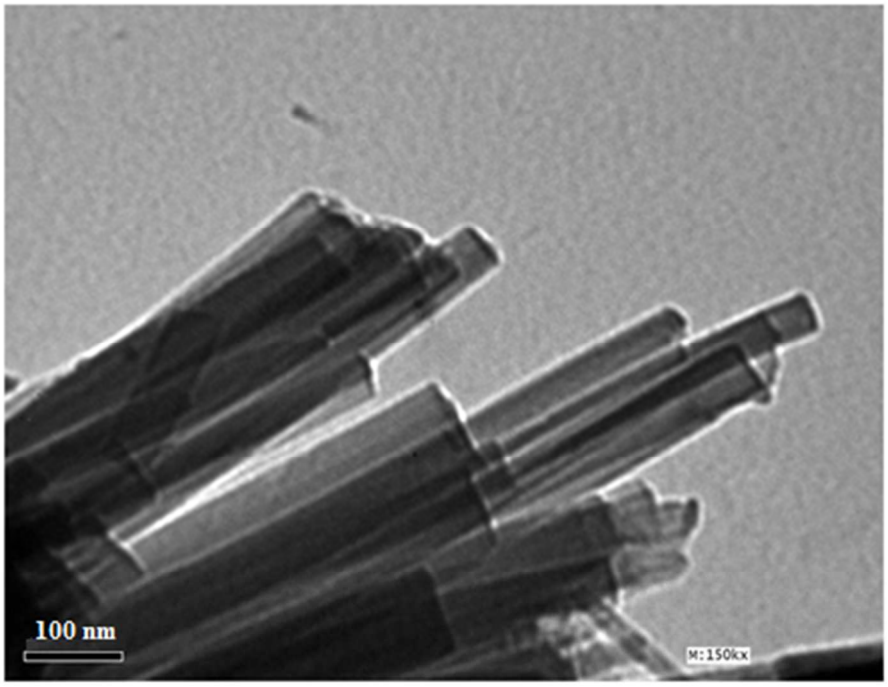

Fig. 2 TEM image of prepared TiO_x nanotubes

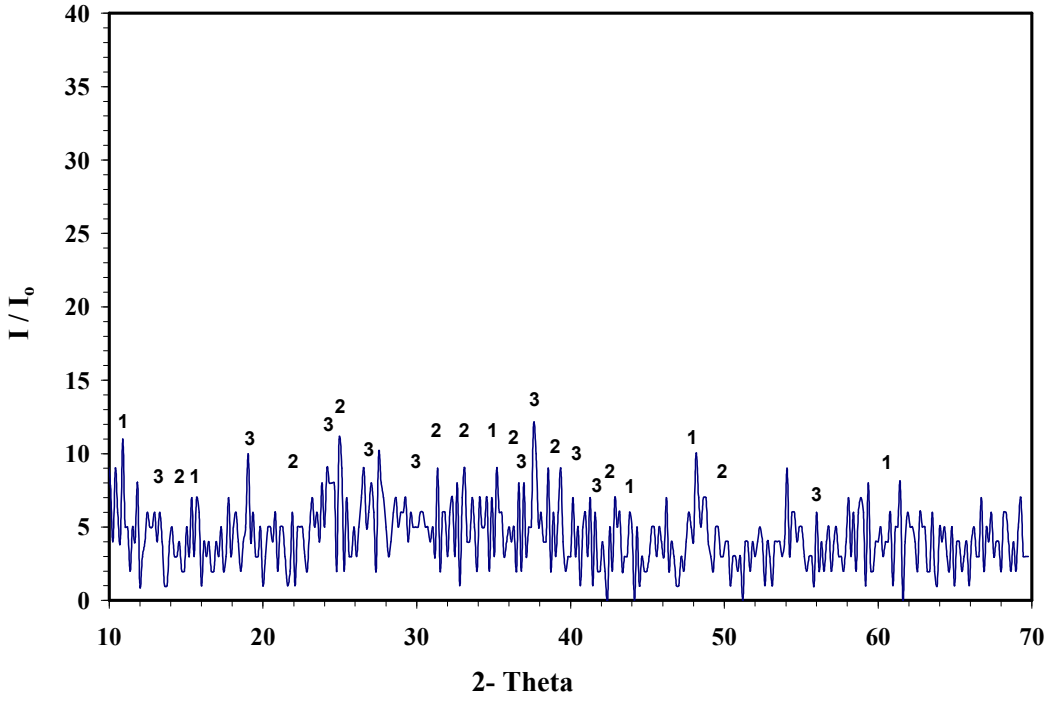

Fig. 3 XRD patterns of $DTiO_xNTs$ where (1) $Na_2Ti_3O_7$, (2) $Na_4Fe_2O_5$, (3) $Na_2Ti_9O_{19}$, (4) $Ti_2Fe_2O_7$

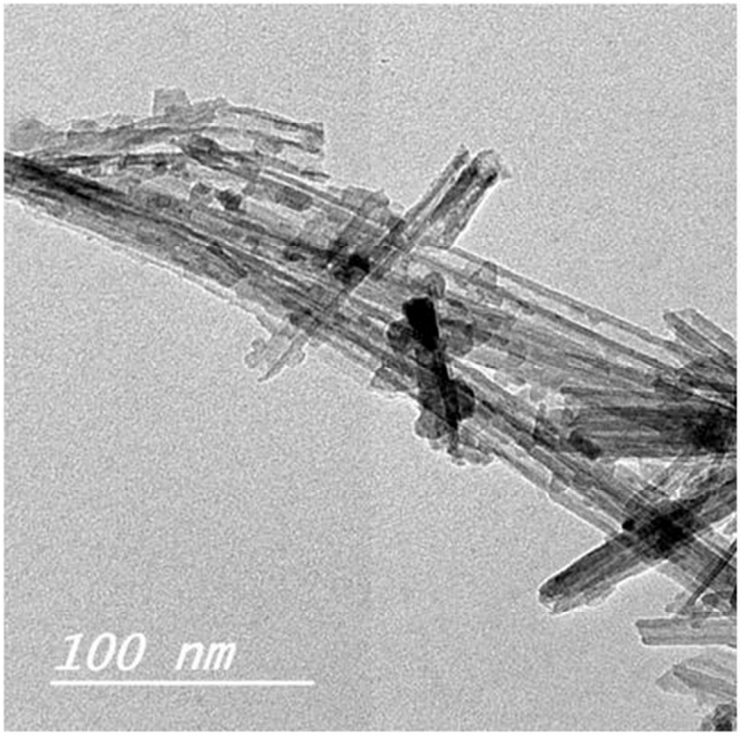

Fig. 4 TEM image of DTiO$_x$NTs

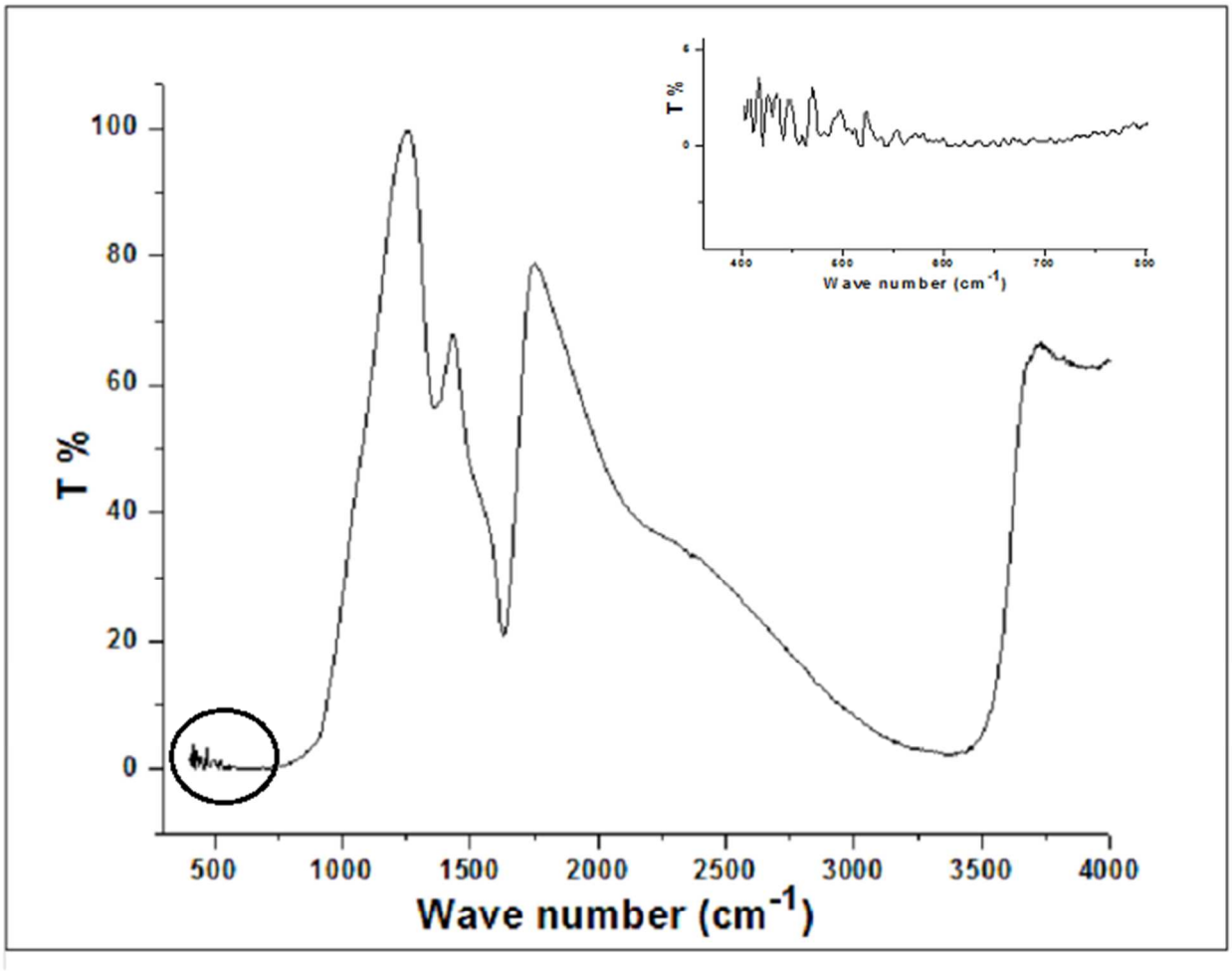

Fig. 5 IR spectra of DTiO$_x$NTs

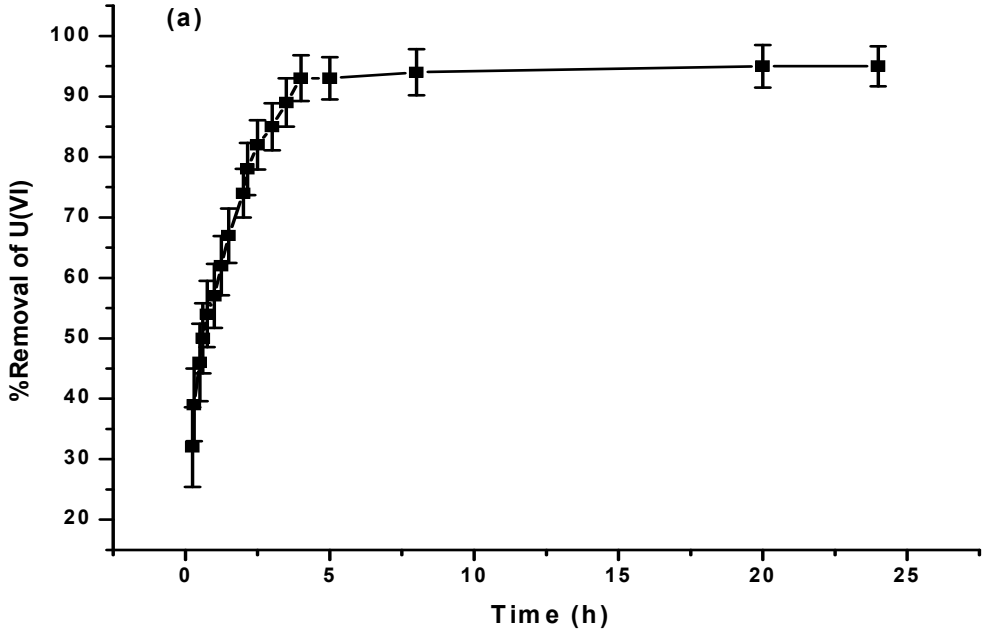

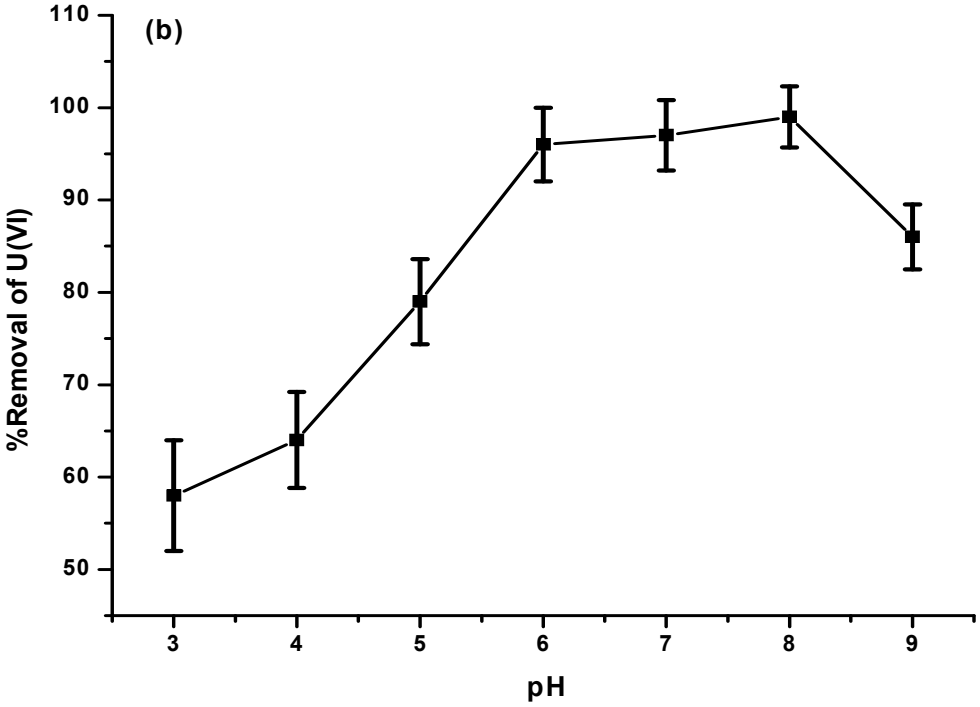

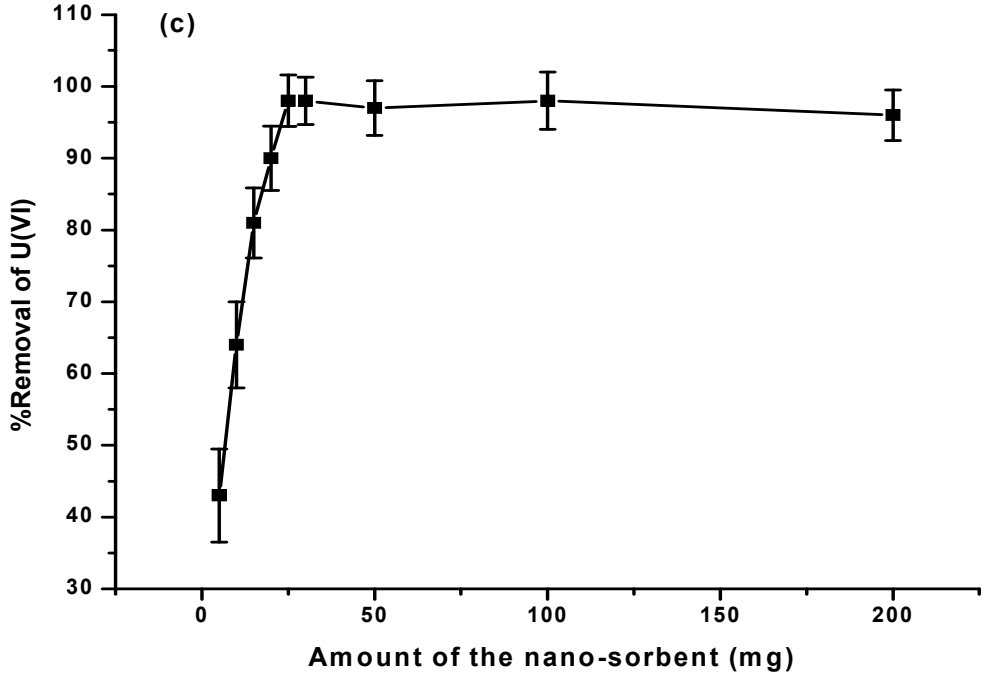

Fig. 6 Influence of some parameters on U(VI) extraction by DTiOxNTs using batch mode: (a) Effect of contact time (20 mg DTiOxNTs, 100 mL sample volume, 100 mg L^{-1} U(VI), pH 6), (b) Effect of pH (20 mg DTiOxNTs, 100 mL sample volume, 100 mg L^{-1} U(VI), 4 h extraction time), and (C) Effect of amount of DTiOxNTs (100 mL sample volume, 100 mg L^{-1} U(VI), pH 6, 4 h extraction time).

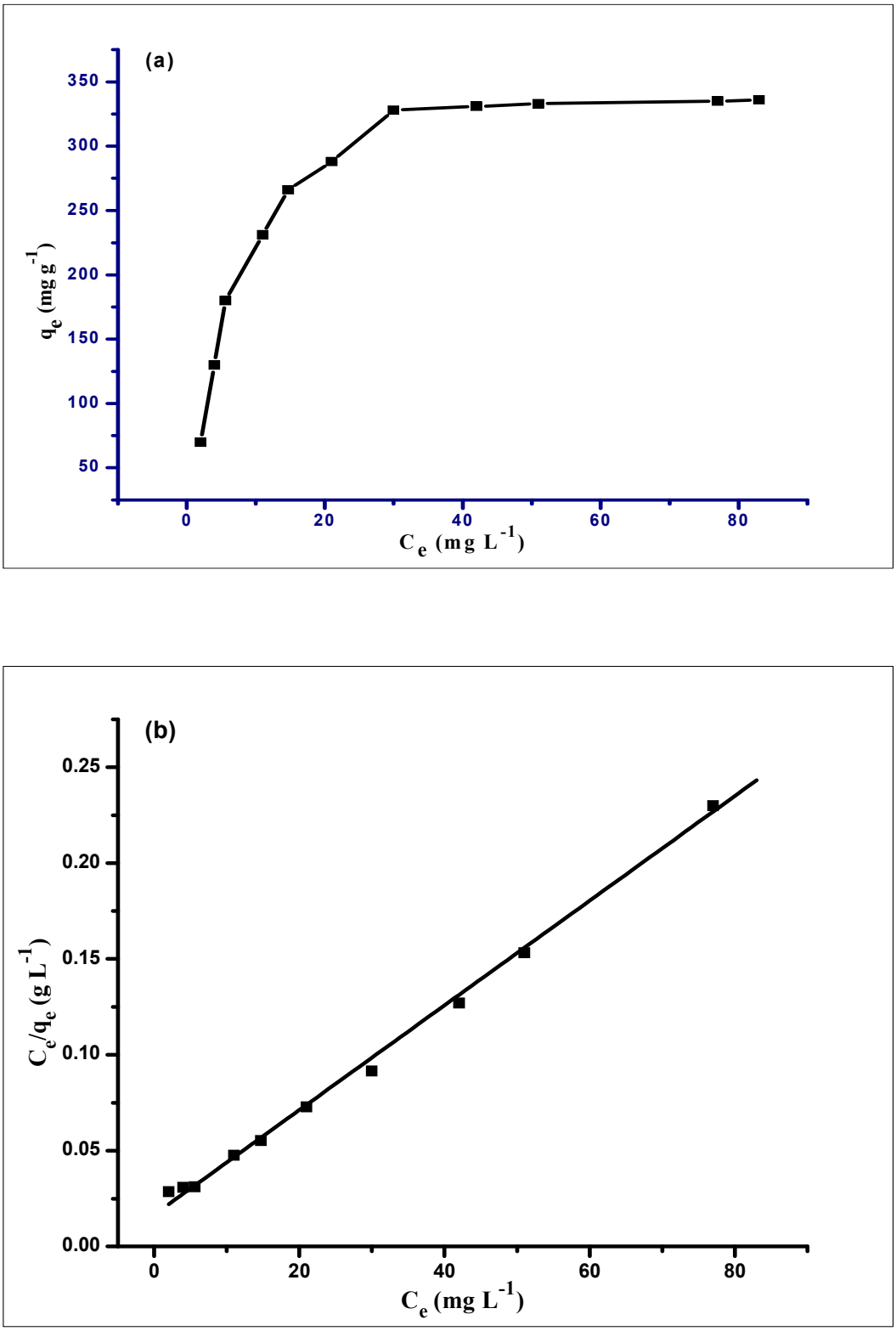

Fig. 7 (a) Adsorption isotherm and (b) linear Langmuir plots for U(VI) onto DTiOxNTs.

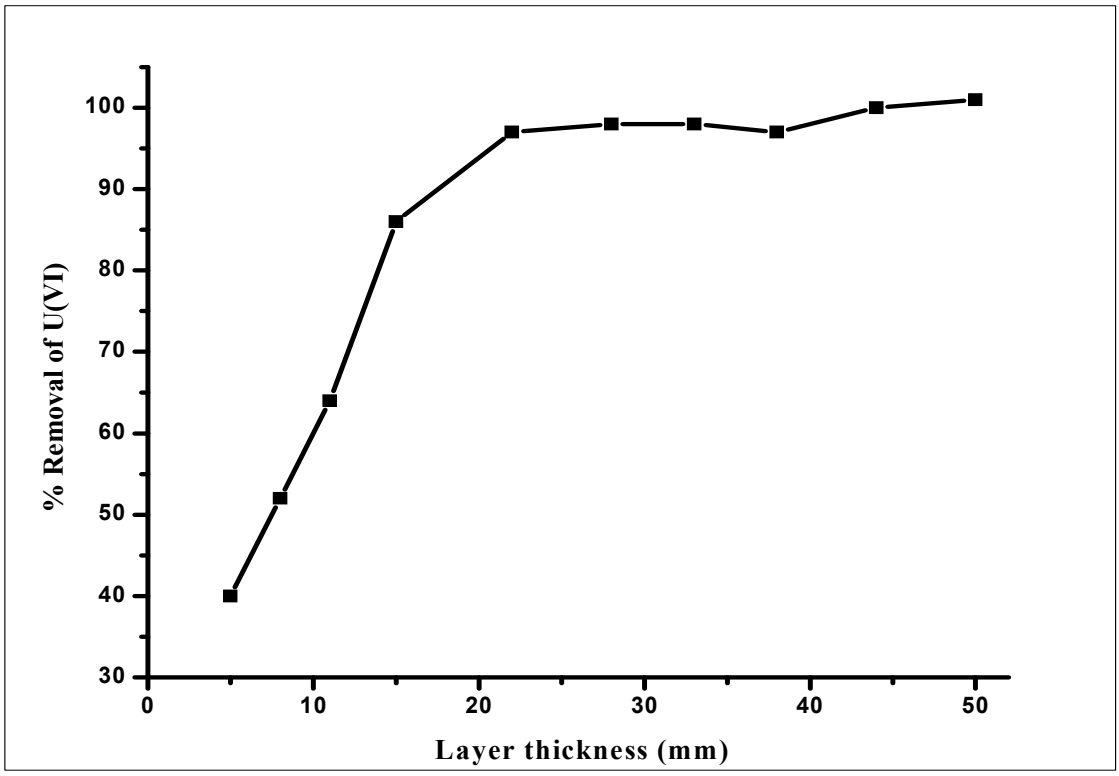

Fig. 8 Effect of layer thickness on adsorption of U(VI), in column system.

Table 1

The operation conditions for ICP-OES determination of U(VI)

RF Power	1350 W
Nebulizer gas flow rate	0.45 L min^{-1}
Auxiliary gas flow rate	0.2 L min^{-1}
Plasma gas flow rate	15 L min^{-1}
Pump rate	2.5 ml min^{-1}
Sample uptake rate	2.5 ml min^{-1}
Plasma viewing	Axial
Peak processing Mode	Peak area
Delay time	7 sec
Integration time	3 sec
Replicates	3
Wavelength	385.958 nm

Table 2

Comparison of U(VI) sorption capacity of DTiO$_2$NTs with other sorbents

Sorbents	pH	q_m (mg g^{-1})	Ref
Graphene oxide-polypyrrole composites	5	147.06	[46]
Carboxymethyl cellulose grafted on multiwalled carbon nanotubes	5	126.00	[47]
Graphene oxide nanosheets	5	97.50	[48]
Magnetic yolk-shell iron oxide@magnesium silicate microspheres	5.5	242.50	[49]
Amidoximated magnetite/graphene oxide composites	5	284.90	[50]
Magnetic ion-imprinted composite	4	354.85	[51]
manganese dioxide-iron oxide-graphene magnetic nanocomposite	6	108.7	[52]
TiO_2 nanotubes	6	277	The present study
TiO_2 nanotubes decorated with $CuFe_2O_4$	6	366	

Table 3

Effect of type, concentration and volume of eluting acid on recovery of U(VI) (n=3)

Eluent	Volume	%Removal of U(VI)
0.1 mol L^{-1} HNO_3	2	62.4±3.6
	5	68.6±4.7
0.2 mol L^{-1} HNO_3	2	71.0±5.5
	5	78.3±3.2
0.5 mol L^{-1} HNO_3	2	82.5±4.7
	5	84.9±4.5
0.1 mol L^{-1} HCl	2	74.2±3.3
	5	83.0±4.2
0.2 mol L^{-1} HCl	2	85.4±3.9
	5	90.2±3.7
0.5 mol L^{-1} HCl	2	91.8±4.1
	5	97.2±2.5

Table 4

Effect of different anions and cations on the sorption recovery of U(VI) on DTiO$_2$NTs

Ion	Tolerable ratio Ion/U(VI)	Extraction (%)	RSD * (%)
Li^+	1000	96.5±3.3	2.7
Na^+	1000	97.1±3.6	3.0
K^+	1000	99.0±2.0	1.8
Mg^{2+}	500	98.6±2.6	2.2
Ca^{2+}	500	101.3±2.8	2.8
Co^{2+}	200	98.5±2.3	1.5
Zn^{2+}	200	95.0±3.8	2.1
Pb^{2+}	200	96.4±3.5	2.8
Cd^{2+}	200	98.0±2.9	1.7
Cu^{2+}	200	100.1±2.8	2.0
Fe^{2+}	200	99.0±2.7	2.7
Fe^{3+}	200	99.5±1.9	3.1
Al^{3+}	200	95.5.±3.3	1.8
Cr^{3+}	200	97.1±2.6	1.5
F^-	1000	98.2±2.2	3.0
Cl^-	1000	96.5±3.0	2.2
Br^-	1000	99.0±2.0	2.6
NO_2^-	1000	95.9±3.2	1.9
NO_3^-	1000	96.3±3.4	3.2
SO_4^{-2}	1000	96.8±2.9	2.4
PO_4^{-3}	500	102.0±2.0	1.4
Citric acid	50	95.6±3.3	3.0
Oxalic acid	50	97.6±2.5	2.2
Humic acid	20	95.8±3.1	2.9
Fulvic acid	20	98.0±2.7	2.6

* RSD of three replicate experiments.

Table 5

Determination of uranium in water and soil samples.

Sample	Added (ng mL^{-1})	Found (ng mL^{-1})	Recovery (%)
River Nile water (Mansoura, Nile Delta)	0	5.70±0.62	-
	2.5	8.13±1.10	97.2
	5	10.60±1.37	98.0
Mediterranean Sea water (Port Said)	0	2.94±0.41	-
	2.5	5.40±1.21	98.4
	5	8.06±1.42	102.4
	Added (µg g^{-1})	**Found (µg g^{-1})**	**Recovery (%)**
Soil samples (Abu Zaabal)	0	1.97±0.46	-
	0.5	2.45±0.65	96.0
	1.0	2.96±0.84	99.0

Table 6

Comparison of analytical features of presented method with other SPE method

Sorbent	Analytical technique	PF [a]	LOD (ng mL^{-1})	Linearity (ng mL^{-1})	Ref.
Mesoporous silica modified with 5-nitro-2-furaldehyde	ICP OES	100	0.30	1-1500	11
Functionalized Fe_3O_4 magnetic nanoparticles with salicylaldehyde groups	ICP OES	1000	0.24	1-5000	12
Salicylaldehyde-modified mesoporous silica	ICP OES	100	0.40	2-1000	13
Phenylarsonic acid-type chitosan resin	ICP OES	25	0.1	1-10	14
Merrifield polymer- octyl(phenyl)- *N,N*-diisobutylcarbamoyl-methylphosphine oxide	Fluorescence spectrophotometer	400	20	-	19
Chloromethylated Calix[4]arene anchored chloromethylated polystyrene	UV–visible	143	6.14	0.1-15	20
Grafting merrifield chloromethylated resin	UV–visible	100	10	-	21
Quinoline-8-ol anchored Chloromethylated polymeric resin	UV–visible	100	5	5-200	22
Duolite XAD761	ICP-MS	30	4.5×10^{-3}	-	16
TiO_x nanotubes decorated with $CuFe_2O_4$	ICP-OES	200	0.12	0.4-1500	The present study